Science Advances
AAAS

advances.sciencemag.org/cgi/content/full/4/12/eaat6387/DC1

Supplementary Materials for

A stability-reversibility map unifies elasticity, plasticity, yielding, and jamming in hard sphere glasses

Yuliang Jin*, Pierfrancesco Urbani, Francesco Zamponi, Hajime Yoshino*

*Corresponding author. Email: yuliangjin@itp.ac.cn (Y.J.); yoshino@cmc.osaka-u.ac.jp (H.Y.)

Published 7 December 2018, *Sci. Adv.* **4**, eaat6387 (2018)
DOI: 10.1126/sciadv.aat6387

This PDF file includes:

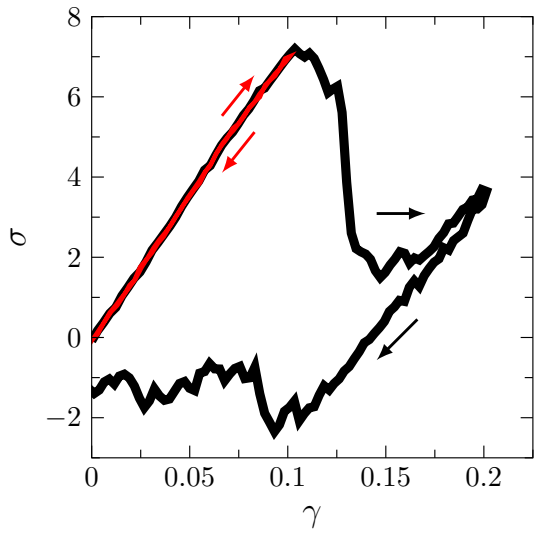

Fig. S1. Singe-realization stress-strain curve for $\varphi_g = 0.655$ and $\epsilon = 0.057$. Single-realization stress-strain curve of the same glass sample as in Fig. 1 at the fixed volume strain $\epsilon = 0.057$ (or $\varphi = 0.62$). The shear strain is reversed at $\gamma = 0.1$ (red) and $\gamma = 0.2$ (black). In contrast to the case in Fig. 1A, the partially irreversible regime is not observed. Note that according to the stability-reversibility map of Fig. 2, the Gardner line will not be crossed over in the CV-S protocol with the volume strain $\epsilon = 0.057$.

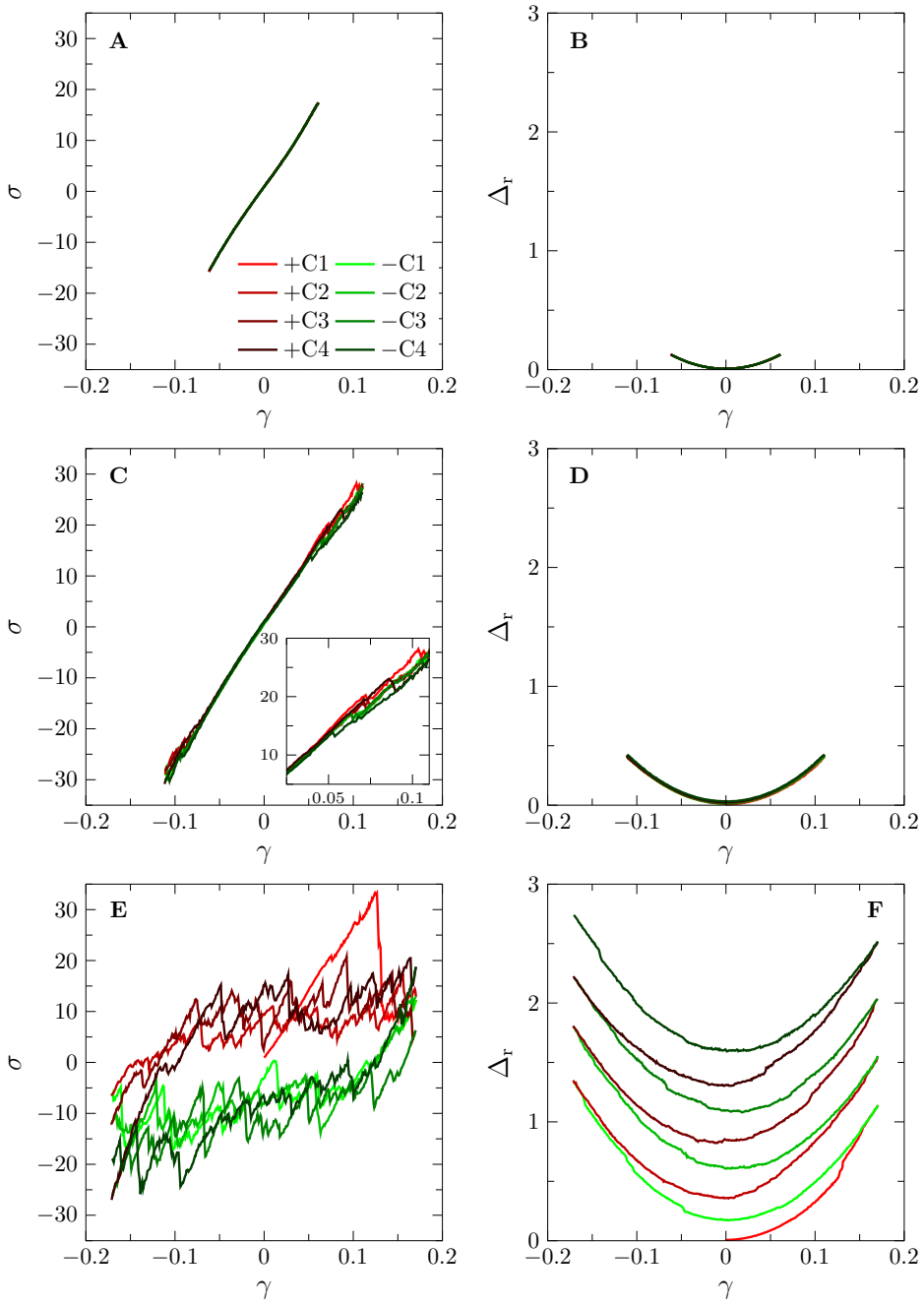

Fig. S2. Multicycle stress-strain curves. Single-realization stress-strain curves of a single sample over four cycles of constant volume shear at $\epsilon = -0.0069$, or $\varphi = 0.66$ (compressed from $\varphi_g = 0.655$). The shear strain is reversed at **(A)** $\gamma = \pm 0.06$, **(C)** $\gamma = \pm 0.11$, and **(E)** $\gamma = \pm 0.17$. The cycle numbers (1, 2, 3, 4) and the shear directions (+ or −) are indicated. In **(C)**, the data for $0.02 \leq \gamma \leq 0.11$ are magnified in the inset to show better the plastic events. The corresponding data of the relative mean squared displacement Δ_r are shown in **(B)**, **(D)** and **(F)**. While in **(B)** and **(D)** the system returns to the initial state, in **(F)** a diffusive behavior of Δ_r, which increases steadily at each cycle, is observed.

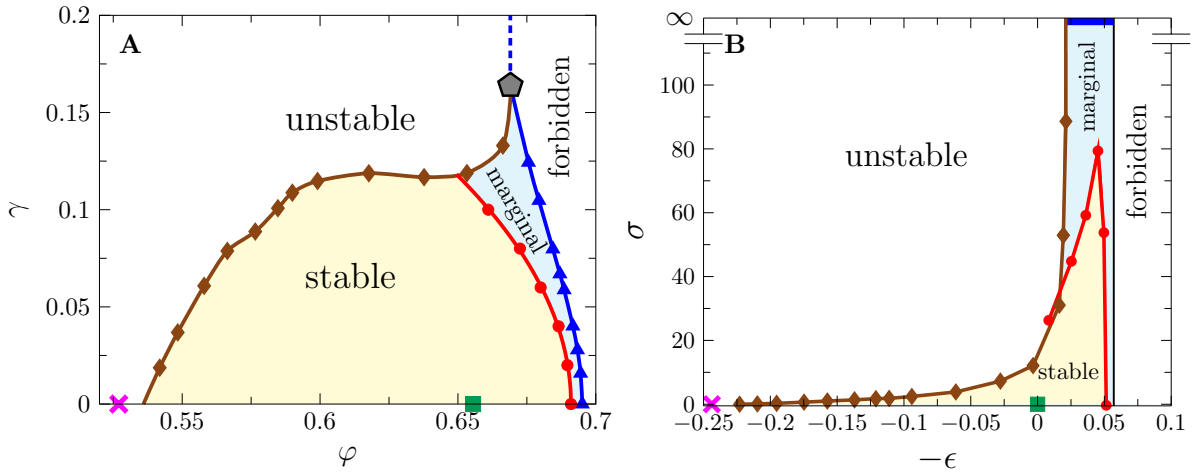

Fig. S3. Other representations of the stability-reversibility map. Stability-reversibility map of the HS glass annealed up to $\varphi_g = 0.655$, as in Fig. 2, but represented in terms of **(A)** volume fraction φ and shear strain γ, and **(B)** volume strain ϵ and shear stress σ. See Fig. 2 for the meaning of symbols.

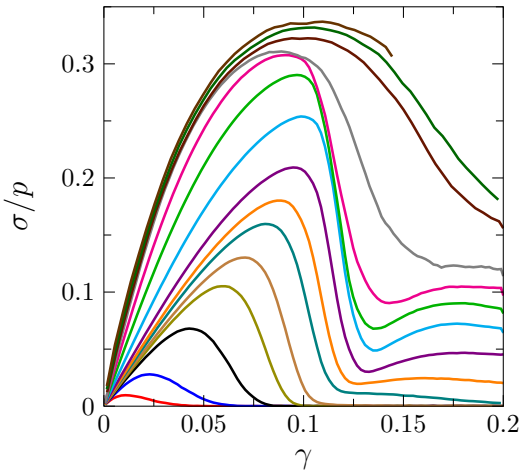

Fig. S4. Rescaled stress-strain curves. The ratio σ/p is plotted as a function of γ in the CP-S protocol, for $p = 14.5$, 15.0, 15.8, 16.5, 17, 18, 19, 21, 27, 40, 65, 160, 1000, 3000, 10000 (from bottom to top), and $\varphi_g = 0.655$.

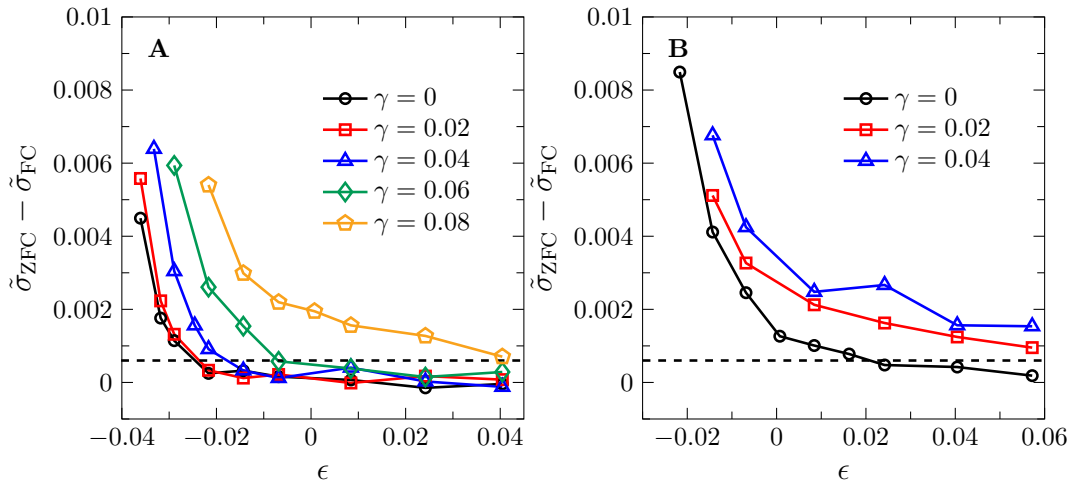

Fig. S5. Determination of the Gardner threshold for other $\varphi_{\rm g}$ The difference between ZFC and FC stresses (rescaled by p, $\tilde{\sigma} = \sigma/p$) as a function of volume strain ϵ for **(A)** $\varphi_{\rm g} = 0.631$ and **(B)** $\varphi_{\rm g} = 0.609$. Data for a few different γ are plotted. The horizontal dashed lines represent the threshold value 0.0006 used to determine $\epsilon_{\rm G}$.

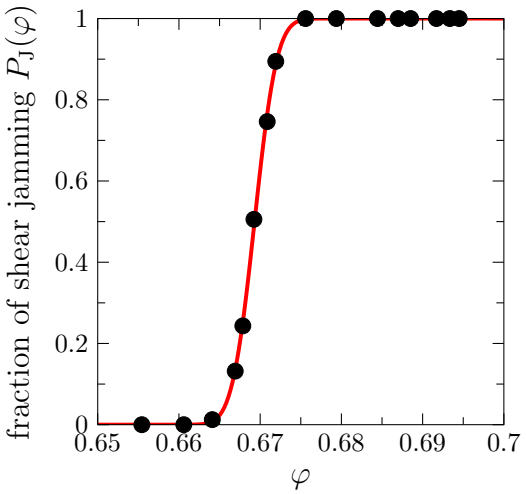

Fig. S6. Determination of the yielding-jamming crossover point. Fraction of shear jamming $P_{\rm J}(\varphi)$ as a function of φ. We use the following criteria to define shear jamming and yielding: a system jams with increasing γ if its pressure p exceeds 10^5; otherwise, if the system can reach the maximum strain $\gamma_{\rm max} = 0.2$ without jamming, then it yields. We use $P_{\rm J}(\varphi)$ to denote the fraction of shear jammed realizations among $N_{\rm r} = 300 - 1200$ total realizations. The data are fitted to the error function form $P_{\rm J}(\varphi) = \frac{1}{2} + \frac{1}{2}{\rm erf}[(\varphi - \varphi_{\rm c})/w]$ (line), where $\varphi_{\rm c} = 0.66931(3)$ and $w = 0.0031(1)$ are fitting parameters.

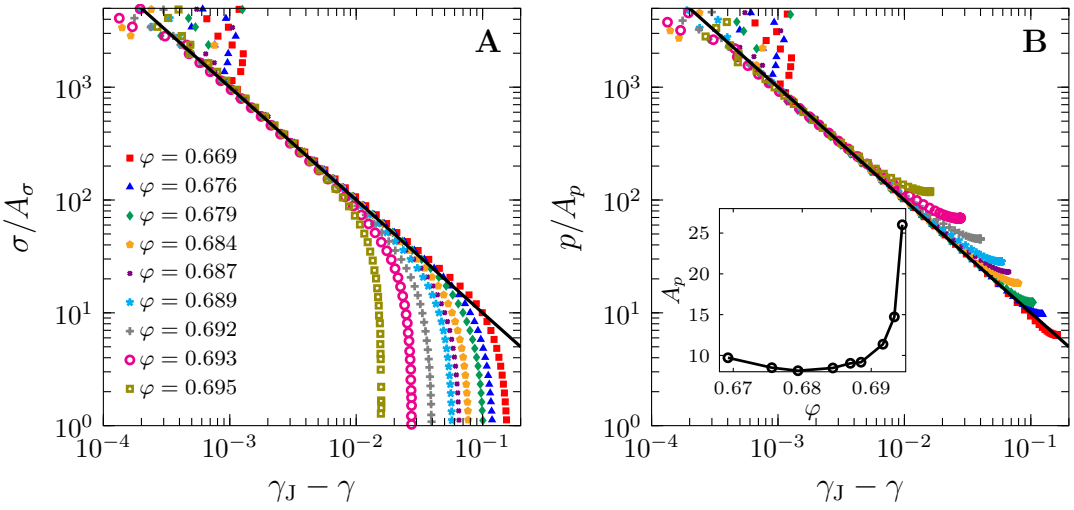

Fig. S7. Free-volume scalings in shear-jamming. The simulation data for different φ obtained by the CV-S protocol ($\varphi_g = 0.655$) are fitted to the free-volume scaling laws **(A)** $\sigma = A_\sigma(\gamma_J - \gamma)^{-1}$ and **(B)** $p = A_p(\gamma_J - \gamma)^{-1}$, where A_σ, A_p, and γ_J are fitting parameters. The values of γ_J are used to determine the shear-jamming line in the main text. We find that $A_\sigma \simeq 2.6$ is nearly independent of φ. The values of A_p are plotted in the inset of **(B)**.

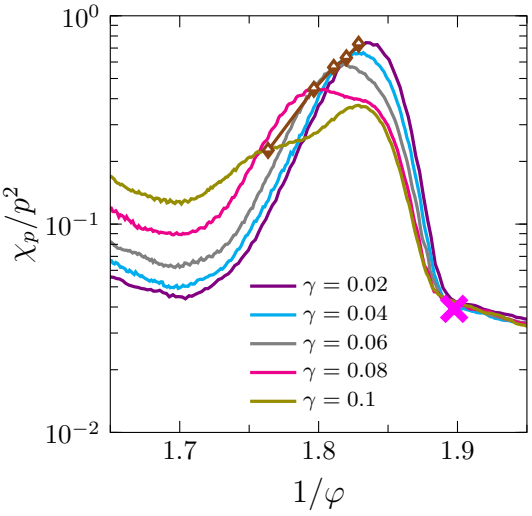

Fig. S8. Pressure susceptibility in the CS-C/D) protocol.
The pressure susceptibility $\chi_p = N(\langle p^2\rangle - \langle p\rangle^2)$ (rescaled by p^2) as a function of $1/\varphi$ for a few different γ in the CS-C/D protocol. In contrast to χ_σ (Fig. 5I), the pressure susceptibility χ_p has two peaks at large γ. The first peak, caused by melting, is independent of γ, while the second one, corresponding to yielding, is at a location consistent with the peak of χ_σ (half filled brown diamonds). The γ-independence of the melting peak in χ_p further confirms that melting is independent of shear strain. For small γ, the two peaks are indistinguishable. The data suggest that the signature of melting only appears in the pressure susceptibility, but not in the stress susceptibility.

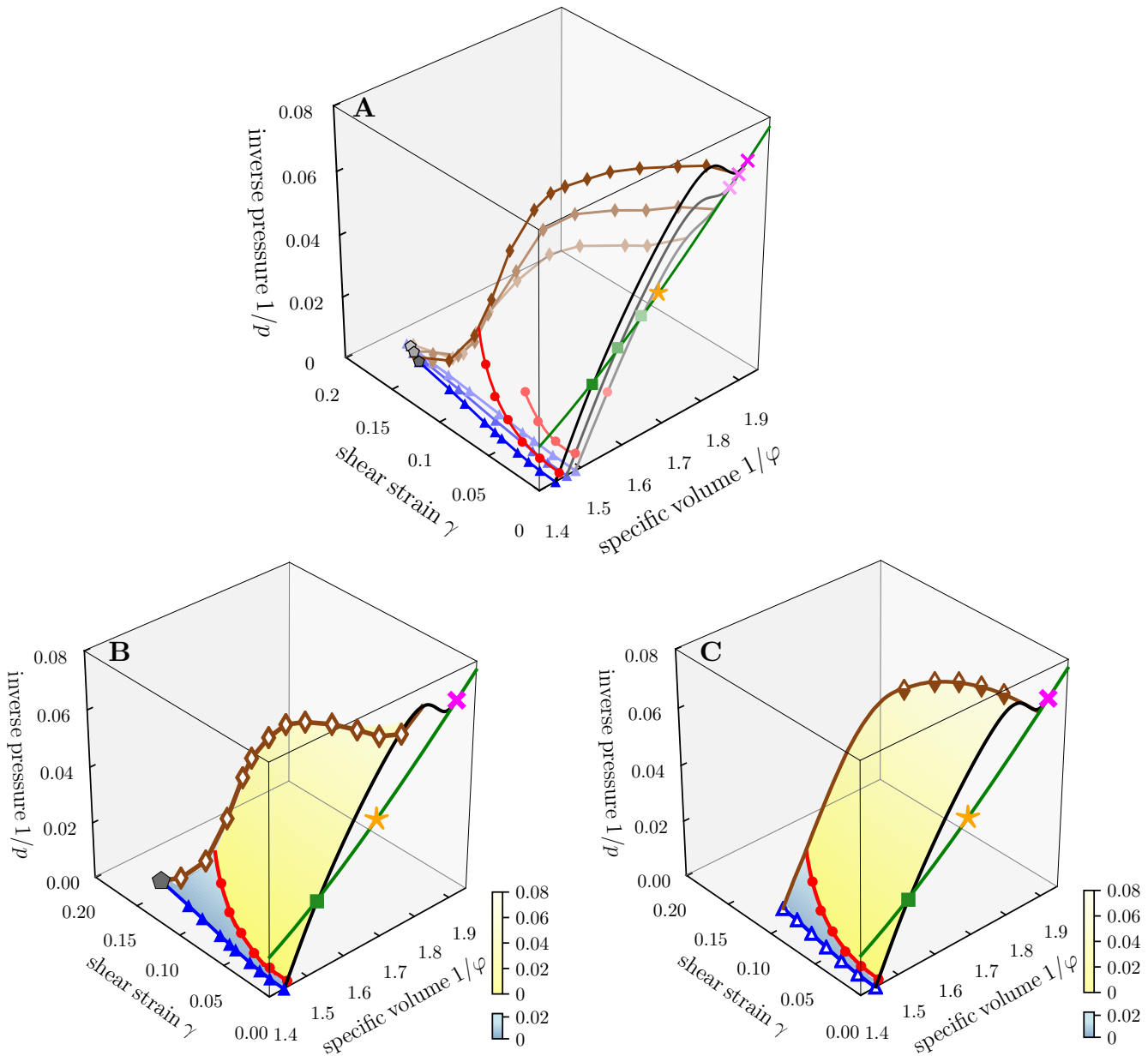

Fig. S9. Dependence of the stability-reversibility map on φ_g and protocols. (A) Three dimensional view of the stability-reversibility maps for $\varphi_g = 0.609, 0.631, 0.655$ (lighter colors represent lower φ_g) obtained by using the CP-S protocol. **(B-C)** The same plot for $\varphi_g = 0.655$, obtained by using the **(B)** CV-S and **(C)** CS-C/D protocols. See Fig. 2 for the meaning of the symbols.

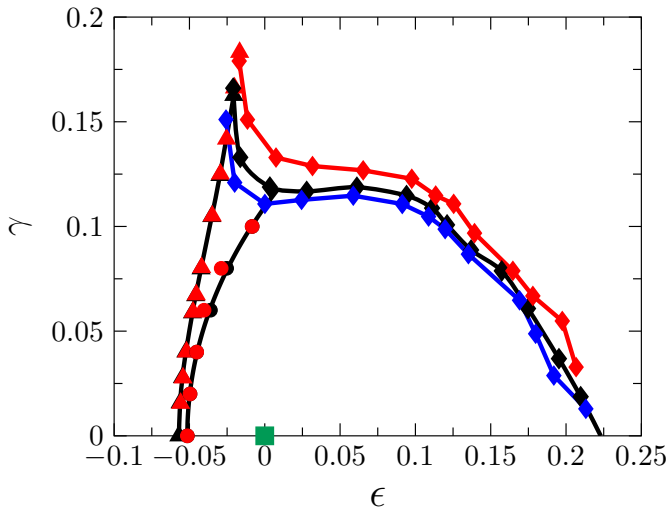

Fig. S10. Dependence of the stability-reversibility map on the system size. Stability-reversibility maps for $N = 500$ (red) and $N = 1000$ (black) systems ($\varphi_g = 0.655$). No appreciable N-dependence is observed for the shear-jamming line and the Gardner line. We also plot the shear-yielding line for $N = 2000$ systems (blue), showing that larger systems have lower yielding strain γ_Y. See Fig. 2 for the meaning of the symbols.

Text S1. Bare and macro shear moduli.
As discussed in the main text, two shear moduli can be defined for glasses: the bare modulus

$$\mu_{\rm bare} = \lim_{N\to\infty}\lim_{\delta\gamma\to 0}\delta\sigma(\varphi_{\rm g};\epsilon,\gamma;N)/\delta\gamma, \tag{S1}$$

and the macroscopic modulus

$$\mu_{\rm macro} = \lim_{\delta\gamma\to 0}\lim_{N\to\infty}\delta\sigma(\varphi_{\rm g};\epsilon,\gamma;N)/\delta\gamma. \tag{S2}$$

According to the mean-field theory [37] in stable glasses $\mu_{\rm bare} = \mu_{\rm macro}$, while in marginal glasses $\mu_{\rm bare} > \mu_{\rm macro}$. In particular, the two shear moduli have different large-p scalings in the marginal phase, $\mu_{\rm macro} \sim p$ and $\mu_{\rm bare} \sim p^{\kappa}$, where $\kappa \sim 1.41574$.

In principle, we expect that the zero-field compression (ZFC) modulus $\mu_{\rm ZFC}$ and the field compression (FC) modulus $\mu_{\rm FC}$ measured in simulations have the correspondence $\mu_{\rm ZFC} \sim \mu_{\rm bare}$ and $\mu_{\rm ZFC} \sim \mu_{\rm macro}$. Ref. [24] shows that the simulation results of three dimensional HS glasses are generally consistent with the above theoretical predictions. In the marginal phase, $\mu_{\rm ZFC}$ and $\mu_{\rm FC}$ clearly have different scalings with p. It was also found that, at large p, $\mu_{\rm ZFC}$ decreases with increasing N or $\delta\gamma$ (note that in simulations, the modulus is measured as $\mu = \delta\sigma/\delta\gamma$, where small, but finite $\delta\gamma$ is used). This shows that the order of limits $N \to \infty$ and $\delta\gamma \to 0$ is important in the definition of shear modulus. If we fix a finite N, then by increasing $\delta\gamma$, $\mu_{\rm ZFC} \to \mu_{\rm FC} = \mu_{\rm macro}$. In fact, one should only be able to detect the $\mu_{\rm ZFC}$ if $\delta\gamma < \delta\gamma_{\rm trigger}$ as discussed in the main text. In this study, we use a small enough $\delta\gamma = 0.002$, as shown in [24], to measure $\mu_{\rm ZFC}$ and $\mu_{\rm FC}$.

In the measurements of the glass equation of state (G-EOS), either the constant volume-shear (CV-S) or the constant pressure-shear (CP-S) protocol corresponds to ZFC. However, we find that the curves σ/p versus γ collapse for large p (see Fig. S4), implying a scaling $\sigma \sim p$, as $p \to \infty$, similar to $\mu_{\rm macro} \sim p$. The result confirms that for large γ, the plasticity events are averaged out in the stress, and therefore only the macroscopic stress $\sigma_{\rm macro}$ can be measured. This is the reason why the G-EOS itself does not encode the signal associated to the Gardner phase.